# DESIGN ANALYSIS FOR THE OPTICAL ELEMENTS OF SOLID-STATE LASER RANGE FINDER

*Zahraa Humam Mohammod*
*College of Engineering – Al-Mustansireah University- Baghdad-Iraq*
*Asst. Lecture*

## Abstract

*Laser remote sensing has become a well-established technique that has been applied in many fields. In particular laser range finders are widely applied in non-contact measurement of distances. Thus, due to their importance, the optical systems associated with laser range finders have been investigated computationally in the present work using a new approach for their design with the aid of Zemax software. Optimization processes have been conducted to determine the most favourable optical properties and hence the design specifications of a beam expander and a beam compressor which both constitute the optical system of a laser range finder. The laser beam source associated with the suggested designs of the optical systems is that of the solid-state Nd:YAG (λ=1.064 μm) since the range finder is intended for operation in the near infrared region. Computations obtained by the Zemax.EE software have been shown that a spot of an optically desirable shape and of radius as small as 54.7 μm can be projected on the detector surface from quite a long distance. The results have been compared with those obtained with the aid of MATLAB program and excellent agreement has been found. The specifications of the optical systems that have been put forward in present investigation can be practically realized.*

## الخلاصة

*أصْبَحَ التحسس بالليزر عن بعُدٍ تقنية راسخةُ طبّقت في العديد مِنْ المجالات . هناك تطبيقات واسعة لمقدرات المدى الليزرية المستخدمة في قياس المسافات. لذلك، بسبب اهمية هذه التقنية تم عمل دراسة حاسوبية للمنظومات البصرية المتعلقة بمنظومة مقدرة المدى الليزرية بأستخدام برنامج زي ماكس. العمليات البصرية المستخدمة تؤدي الى حساب اغلب الخصائص البصرية ولذلك تم تصميم منظومة من موسع الحزمة وجامع الحزمة والذي يكونان النظام البصري لمقدرات المدى الليزرية. ان مصدر الليزر المستخدم في التصميم هو من نوع ليزر الحالة الصلبة وهو Nd:YAG وطوله الموجي هو 1,064 مايكروميتر ويتم تشغيل مقدرة المدى في منطقة الاشعة تحت الحمراء. ان العمليات الحسابية التي تم الحصول عليها بواسطة برنامج زي-ماكس قد بينت ان بقعة الليزر ذات شكل مرغوب به بصريا وبنصف قطر صغير يصل الى 54,7 مايكروميتر ويمكن تسقيطها على سطح الكاشف من مسافة بعيدة. ان النتائج التي تم الحصول عليها من برنامج زي-ماكس تم مقارنتها مع النتائج التي تم الحصول عليها من برنامج MATLAB وقد اظهرت توافقا بين النتيجتين. كما ان مواصفات الانظمة البصرية التي قدمت في البحث التالي قابله للتنفيذ عمليا.*

## 1. Introduction

The process of optical design is both an art and a science. There is no closed algorithm that creates a lens, nor is there any computer program that will create useful lens designs without general guidance from an optical designer. The mechanics of computation are available within a computer program, but the inspiration and guidance for a useful solution to a customer's problems come from the lens designers. A successful lens must be based upon technically sound principles. The most successful designs include a blend of techniques and technologies that best meet the goals of the customer. This final blending is guided by the judgment of the designer [8]

.

### 1.1 Theoretical Basics

The following formulas for lenses in air are based on the behavior of paraxial rays, which are always very close and nearly parallel to the optical axis. In this region, lens surfaces are always very nearly normal to the optical axis, and hence all angles of incidence and refraction are small

#### 1.1.1 focal length

The focal length of a lens is given by the following lens maker's equation: [5]

$$\frac{1}{f}=(n-1)\left(\frac{1}{r_1}-\frac{1}{r_2}\right)+\frac{(n-1)^2}{n}\left(\frac{t_c}{r_1 r_2}\right) \quad \ldots\ldots\ldots\ldots\ldots\ldots\ldots (1.1)$$

where two refracting surfaces of radii $r_1$ and $r_2$ , *tc* is the lens thickness and *n* is the refractive index of the lens material.

$$\frac{1}{f}=(n-1)\left(\frac{1}{r_1}-\frac{1}{r_2}\right) \quad \ldots\ldots\ldots\ldots\ldots\ldots\ldots (1.2)$$

$$\frac{1}{f}=\frac{1}{f_1}+\frac{1}{f_2}-\frac{d}{f_1 f_2} \quad \ldots\ldots\ldots\ldots\ldots\ldots\ldots (1.3)$$

For a system of two lenses of focal lengths $f_1$ and $f_2$, the following expression for the combined effective focal length *f* is the same whether lens separation distance *d* is large or small and whether $f_1$ and $f_2$ are positive or negative.

#### 1.1.2 back focal length

When the focal length is measured from the last vertex of a lens it is referred to the *back focal length* ( $f_b$ ) given by [5],

$$f_b = F''+A_2H''$$
$$= F^{"} - \frac{r2t_c}{n(r2-r1)+t_c(n-1)} \qquad \ldots\ldots\ldots\ldots\ldots\ldots(1.4)$$

Where $F^{"}$ is the rear focal point, $A_2$ is the secondary vertex, and H" is the secondary principal point.

### 1.1.3 F-number

F-number (*F/#*) is the ratio of the paraxial effective focal length calculated at infinite conjugates over the paraxial entrance pupil diameter[2].

$$F = \frac{f}{D} \qquad \ldots\ldots\ldots\ldots\ldots\ldots\ldots\ldots\ldots..(1.5)$$

where *D* is the lens diameter.

### 1.1.4 numerical aperture

Numerical aperture (NA) is the sine of the angle made by the marginal ray with the optical axis. [3]

$$NA = \sin\theta = \frac{D}{2f} \qquad \ldots\ldots\ldots\ldots\ldots\ldots\ldots\ldots...(1.6)$$

### 1.1.5 depth of focus

Depth of focus (DOF) is a small range of axial distance around the image plane in which image appears to be equally sharp for a given object distance. It is given by [6]:

$$\text{DOF}=4\lambda\left(\frac{f}{D}\right)^2 \qquad \ldots\ldots\ldots\ldots\ldots\ldots(1.7)$$

where *D* is the lens diameter, and λ is the wavelength of light

### 1.1.6 field of view

FOV is the angle subtended by the source producing the maximum usable image size; it is given by [2],

$$\text{FOV}= 2\tan^{-1}\left(\frac{UIH}{EFL}\right) \qquad \ldots\ldots\ldots\ldots(1.8)$$

Where UIH is the usable image height

### 1.1.7 Snell's law of refraction

Snell's law, is important in optical system design. Let $\theta_1$ and $\theta_2$ are the angles of incidence and refraction at the interface between media of refractive indices $n_1$ and $n_2$. Snell's law states that incident and refracted rays are coplanar with the normal and that

$$n_1 \sin\theta_1 = n_2 \sin\theta_2 \qquad \text{.....(1.9)}$$

## 1.2 Aberrations of Optical Systems

Aberration is the problem of all image forming systems. The departure of an actual image from its real shape and position (gaussian image) are known as aberrations.There are two types of lens aberrations: (a) monochromatic aberrations (or Seidel aberrations) which are These aberrations are present even for light of a single wavelength. The primary aberrations of any rotationally symmetric system can be specified by the following five coefficients: spherical aberration, coma, astigmatism, curvature of field, and distortiondue to wide angle of incidence and large radial height, and (b) chromatic aberration which is due to the dispersion of composite light [7].

## 1.3 Optical Lens Materials

The index of refraction of the glass can be obtained with the aid of the following *dispersion formula* [3]

$$n = \left[ \frac{B1\lambda^2}{\lambda^2 - C1} + \frac{B2\lambda^2}{\lambda^2 - C2} + \frac{B3\lambda^2}{\lambda^2 - C3} \right]^{1/2} \qquad \text{.....(1.10)}$$

where $\lambda$ is the wavelength of light and *B1* through *C3* are constants given by the glass manufacturer for each type.

## 1.4 Paraxial Ray Tracing

the refracted ray is specified by *hj* and *u' j* so that the incidence heights and convergence angles are generalized coordinates of the ray as it passes through the optical system [9], therefore

$$n'_j u'_j - n_j u_j = -h_j K_j \qquad (1.11)$$

where $$K_j = (n'_j - n_j)c_j \qquad (1.12)$$

and

$$h_{j+1} = h_j + d'_j u'_j \qquad (1.13)$$

$$EFL = \frac{-h_1}{u_j} \quad , \quad f_b = \frac{h_j}{u_j} \qquad (1.14)$$

## 2. Design Considerations

The suggested systems consist of refracting and/or reflecting components in order to expand or compress a beam of light. As one would expect, each system has its own advantages and disadvantages concerning, for instance, its fabrication process, simplicity, compatibility, and cost Figure (2.1) shows seven designs suggested for image forming optical systems that have been analyzed with the aid of Zemax software before selecting the desirable design. It is seen that system (a) is simple in design and construction but suffers from spherical aberration which is the major disadvantage. Systems (b), (c), and (d) exhibit astigmatism and coma aberrations due to the off-axis alignment. System (e) has the disadvantage of large length which is undesirable in compact optical systems. Systems (e) and (f) constitute a doublet lens to minimize the aberration; this doublet needs to be cemented with some other material. Systems (c) and (g) have the disadvantage of reducing the image intensity due to the limited number of rays coming from the source. The disadvantages of the above systems have been overcome by proposing the designs illustrated in figure (2.2).

The optical systems shown in figure (2.2) perform the process of expanding (figure 2.2 a) and compressing (figure 2.2 b) a laser beam in the transmitter and receiver parts of the range finder system respectively. The two designs are Galilean in form i.e. there is no internal focus. The overall length of the beam expander and beam compressor does not exceed 12 cm each in order to meet the specification requirements for a compact laser range finder. Each system in figure (2.2) consists of two lenses in order to make the design as simple as possible and would maintain the required performance. The two systems are intended for operation in the infrared region of the electromagnetic spectrum. In fact both systems are aimed to work within the wavelength of the Nd:YAG laser since it is commonly used in laser range finder systems. The material lenses is of BK7 type of glass which has the advantage of low cost and desirable optical parameters.

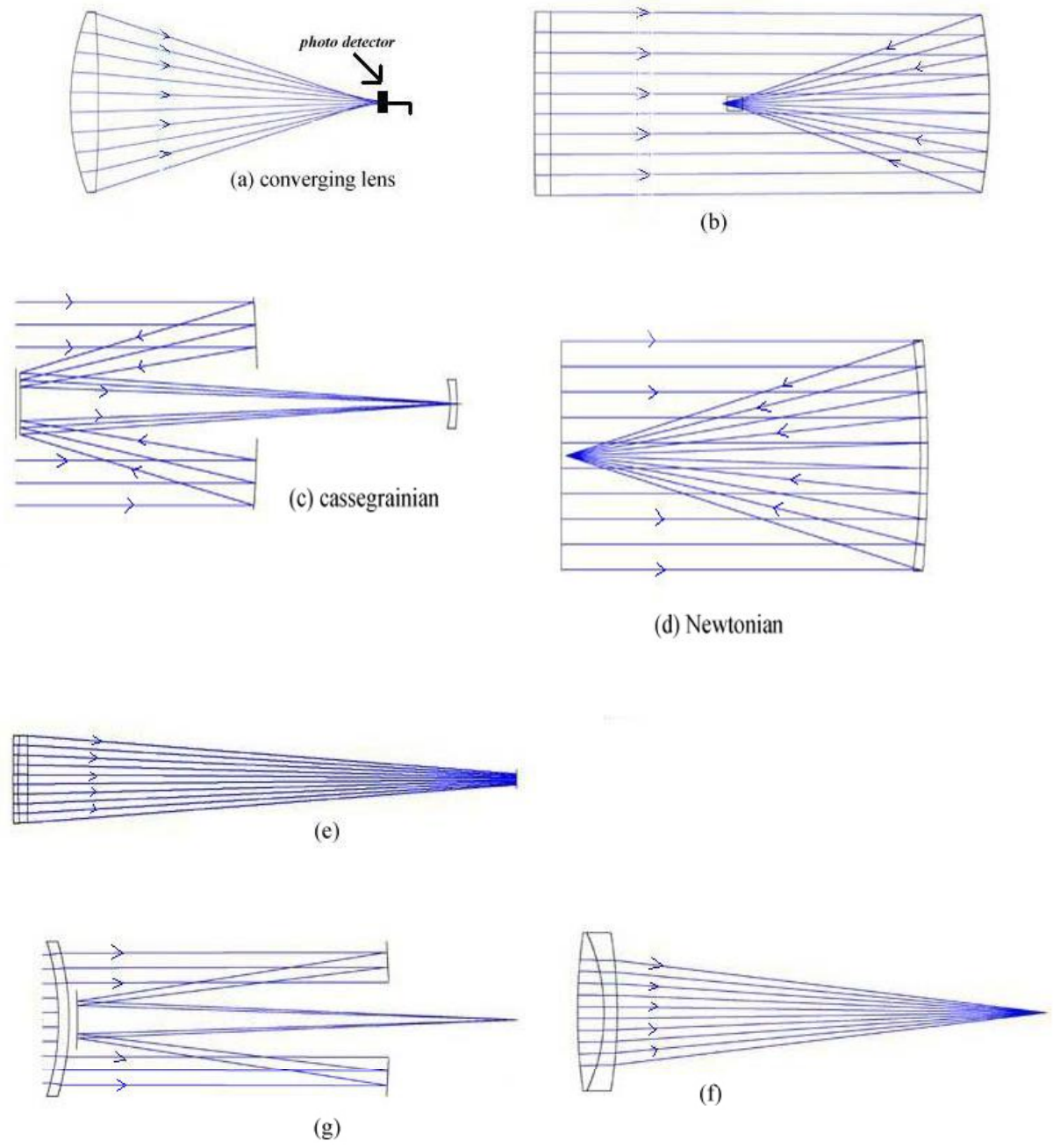


***Figure (2.1) Suggested designs for some optical systems determined by Zemax program***

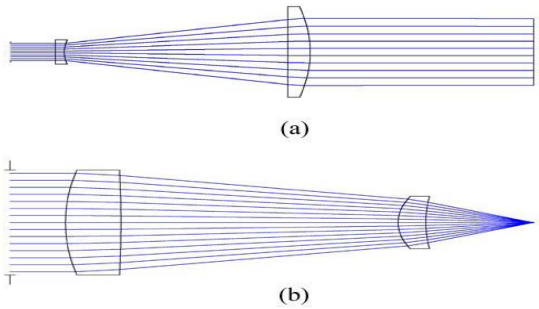


***Figure 2.2 Transmitter and receiver optics of the laser range finder.(a) beam expander,(b) beam compressor***

The Zemax program uses the matrix formula to represent any optical system. In the present investigation Zemax has been used to determine the design of the optical systems for the IR range finder.

# 3.Result and discussion

## 3.1 Beam Compressor

### 3.1.1 Optimization process

A design for a beam compressor has been put forward with the aid of Zemax program. It consists of two BK7 lenses; one is double convex of radii $R_1$ and $R_2$ and the other is concavo-convex of radii $R_3$ and $R_4$ as shown in figure (2.2b). The figure shows the optical path of the laser beam passing through the beam compressor system where the least square method has been used for focusing a perfect image quality of energy distribution. This image represents the input to the detector surface. All the relevant data concerning the system are listed in table (3.1). The lenses data have been taken from examples found in the literature [4]. The following is a description of the titles of the columns and rows of this table.

**Table (3.1) Initially proposed data of beam compressor lenses(all dimension are in millimeter)[4].**

| Surface | Radius | Thickness | Glass | Semi diameter |
|---|---|---|---|---|
| OBJ | Infinity | Infinity | | 0 |
| STO | Infinity | 10 | | 15 |
| 2 | 70 | 10 | BK7 | 20 |
| 3 | -480 | 50 | | 20 |
| 4 | 15 | 5 | BK7 | 10 |
| 5 | 45 | 20 | | 10 |
| IMA | Infinity | | | 0 |

The abbreviations OBJ, STO, and IMA listed in Surface column represent the object, stop aperture, and image respectively. The data listed in table (3.1) represent the proposed values of the parameters before the process of optimization. With the aid of ray tracing analysis and the data given in table (3.1), it has been found that the radius of the spot is 682.4157 μm; a considerably large value. Computations on the aberrations have shown that the value of the total aberrations is mainly dominated by that of the spherical aberration. Thus apart from spherical aberration, the total value of other aberrations has been neglected since it is found to be insignificant. The spherical aberration before optimization is 0.24785 mm. An optimization process has been carried out using least square method concerning the radii of curvature $R_1$, $R_2$, $R_3$, and $R_4$ in order to achieve the lowest possible spot size and the associated aberrations. The process begins by varying $R_1$ and keeping $R_2$, $R_3$, and $R_4$ constants until the lowest spot size is obtained as indicated in figure (3.1). The region of minimum R1 has been enlarged to clarify it. The spot diagram under this condition is shown in figure (3.2). By keeping $R_1$ constant at this optimized value (62.9934 mm) together. with the previous values of $R_3$ and $R_4$, the radius of curvature $R_2$ has been varied until the smallest spot size has been achieved at $R_2$ =-495.814 mm as shown in figure (3.3). The negative sign is an indication for a concave surface. Figure (3.4) depicts the shape of the spot when both $R_1$ and $R_2$ are optimized. A similar procedure has been carried out with regard to $R_3$ by keeping constant the optimized values of $R_1$ and $R_2$ together with the original value of $R_4$. The spot diagram at the optimized value of $R_3$ (15.529 mm) is shown in figure (3.5). The perimeter of the spot surface shows distortion due to the presence of aberration in the system. The final spot diagram shown in figure (3.6) is obtained at the optimized value of $R_4$ shown in figure (3.7) with the aid of the constant optimized values of $R_1$, $R_2$, and $R_3$. These results are listed in table 3.2. The spot surface shape shown in figure (3.6a) indicates that the distortion. previously appeared at its perimeter has been reduced by the optimization process. The relative intensity scale (figure 3.6b) indicates that the maximum intensity is found at the center of the spot.

***Table 3.2 Spot size, spherical aberration, and the corresponding optimized radii of curvature***

| **Optimized Radius of Curvature (mm)** | Spot Size Radius( μm ) | Spherical Aberration **(mm)** |
|---|---|---|
| $R_1$ **= 62.9934** | **452.1834** | **0.2201** |
| $R_2$ **= -495.814** | **265.713** | **0.22** |
| $R_3$ **= 15.529** | **61.14656** | **0.213** |
| $R_4$ **=45.418** | **54.72743** | **0.21094** |

The final result for the spot size (54.727 μm) with such small spherical aberration (0.21 mm) represents the most favorable parameter to be obtained for a beam compressor optical system. The design data of this system are listed in table 3.3. The lens data after the process of optimization are given in table 3.4. The spot diagrams are depicted in figure (3.8)here the relative intensity profile is drawn beside the interferogram. The distortion at the edge of the 3 – D diagram of the wave front suggests that one should concentrate on its peak region. The edges of the wave front may be eliminated by means of an aperture of diameter less than 100 μm placed close to the detector; this is deduced from the value of the semi – diameter of the image given in table(3.4)

***Table 3.3 General lens data***

| | |
|---|---|
| **Number of surfaces** | 6 |
| **Stop number** | 1 |
| **Lens units Millimeter** | **Millimeter** |
| **System aperture** | **30 mm** |
| **Glass catalog** | **Infrared OLD-SCHO** |
| **Effective focal length** | **48.55859 mm** |
| **Back focal length** | **20.03082 mm** |
| **Total track** | **94.51 mm** |
| **f-number F/#** | **1.61862** |
| **Numerical aperture NA** | **0.2951443** |
| **Stop radius** | **15 mm** |
| **Entrance pupil diameter** | **30 mm** |
| **Entrance pupil position** | **0 mm** |
| **Exit pupil diameter** | **66.28591 mm** |
| **Exit pupil position** | **107.8125 mm** |
| **Wavelength** | **1.0641 μm** |

***Table 3.4 Final data of beam compressor lenses (all Dimensions are in millimeter).***

| Surface | Radius | Thickness | Glass | Semi - Diameter |
|---|---|---|---|---|
| **OBJ** | **Infinity** | **Infinity** | | 0 |
| **STO** | **Infinity** | 10 | | 16 |
| 2 | **62.9934** | 10 | BK7 | 16 |
| 3 | **-495.814** | 50 | | 15 |
| 4 | **15.52968** | 5 | BK7 | 8 |
| 5 | **45.41775** | **19.51** | | 8 |
| IMA | **Infinity** | | | **0.0547** |

### 3.1.2 Paraxial lens formulas

A computer program has been written in MATLAB for calculating the parameters of the beam compressor optical system using the paraxial lens formulas. The following calculated parameters have been compared with those determined computationally by Zemax program and the result written in table (3.5).

**Table(3.5)**

| Paraxial lens formuls | Zemax result | MATLAB result | Accuracy |
|---|---|---|---|
| **Effective Focal length EFL** | 48.55859mm | 48.070023 | 1% |
| **back focal length** | -20.03082 | -20.03082 | 3.33738*10-6% |
| **focal-number** | 1.61468 | 1.602334 | 0.8% |
| **numerical aperture** | 0.2951443 | 0.312045 | 5.7% |
| **depth of focus** | 11.09725um | 10.928199um | 1.52% |
| **field of view** | 2.555335 | 2.560906 | 0.22 |

### 3.1.3 Ray tracing analysis

The paraxial ray tracing analysis includes the image height through the surfaces of the beam compressor system in the direction of laser propagation and the angles of paraxial rays emitted from the source through the optical system to achieve the final image or spot on the detector surface. The image height and angle of incidence obtained from Zemax program are listed in table 3.6. It is seen, as one would expect, that the height of the image decreases as the beam propagates towards the image position.

**Table 3.6 Zemax ray tracing results**

| Surface | Image Height (mm) | Tracing Angle (rad) |
|---|---|---|
| **OBJ** | Infinity | 0 |
| **STO** | 15.0000 | 0 |
| 2 | 15.0000 | -0.0798169 |
| 3 | 14.19928 | -0.1339312 |
| 4 | 7.441837 | -0.2433048 |
| 5 | 6.187624 | -0.2951443 |
| IMA | 0.1608841 | -0.2951443 |

By using equations (1.11) – (1.13) and with the aid of Matlab software program the image height and the angle of incidence have been recomputed.The results are listed in table 3.7.

***Table 3.7 Calculated ray tracing results***

| Surface | Image Height (mm) | Tracing Angle (rad) |
|---|---|---|
| **OBJ** | Infinity | 0 |
| **STO** | 15.0000 | 0 |
| 2 | 15.0000 | -0.080072 |
| 3 | 14.199276 | -0.135149 |
| 4 | 7.441837 | -0.250843 |
| 5 | 6.187624 | -0.308905 |
| IMA | 0.160884 | -0.308905 |

A comparison between the corresponding column of tables 3.6 and 3.7 indicates that their accuracy is extremely high particularly that of the image height. As an example, the percentage error concerning the ray tracing angle is illustrated in figure (3.9). It is seen that the percentage error decreases steeply to very low values with decreasing angle. The various parameters of the beam compressor optical system, which have been determined by different methods, have shown excellent agreement. Thus this high accuracy may be considered as a verification of the results and a justification for the approach that has been followed in the present investigation.

## 3.2 Beam Expander

### 3.2.1 Optimization process

The proposed design for the beam expander that is aimed to be optimized consists of two glass lenses of type BK7. One lens is plano – concave of radii R1 and R2 and the other is plano – convex of radii R3 and R4 as shown in figure 2.2a. The function of each lens is illustrated in figure (2.2.a) which shows the path of the laser beam traversing the beam expander optical system. In order to carry out the optimization process for the design of the beam expander, initial specification data published in the literature have been considered Table 3.7 shows the proposed data for initiating the process of optimization. The abbreviations and terms in the columns and rows of table 3.7 are the same as those of table 3.1.

**Table 3.8 Initial data of beam expander lenses (all dimension are in millimeter)**

| Surface | Radius | Thickness | Glass | Semi-Diameter |
|---|---|---|---|---|
| **OBJ** | Infinity | Infinity | | 0 |
| **STO** | Infinity | 10 | | 2.5 |
| **2** | Infinity | 2 | BK7 | 4 |
| **3** | 7 | 50 | | 4 |
| **4** | Infinity | 5 | BK7 | 13 |
| **5** | -20 | 50 | | 13 |
| **IMA** | Infinity | | | 2 |

The Zemax computer program has been applied for the optimization process. The least square method has been used for minimum divergence performance of the incoming beam from the laser source. The divergence angle resulted from the computations by using the data listed in table 3.8 is found to be –0.12577 radian. The minus sign indicates for the divergence of the beam. This value of the divergence angle is not good enough for long distance laser pulse transmission. It is mentioned in the literature that the divergence angle for the transmitted beam in laser range finders should not exceed 5mrad [1].

When the divergence angle is very small, the performance of the optical system is considered to be of high standard. An optimization process has been carried out concerning the radii of curvature R2 and R4 of the lenses shown in figure (3.10) in order to achieve the lowest possible divergence angle. The radii of curvature R1 and R3 are infinite; both have been kept constant at this value in order to fulfill the performance requirements of the Galilean type beam expander. The process of optimization begins by varying R2 and keeping R4 constant at its initial value of 7 mm until the lowest divergence angle is obtained as shown in figure (3.11). It is seen that as R2 is increased the divergence angle decreases monotonically to values where it tends to diminish. The region at which the divergence angle diminishes with increasing R2 has been enlarged for clarification as plotted in figure (3.12). This figure suggests that a value of 10 mm for R2 gives the lowest possible divergence angle of –0.107 mrad.

The positive sign of R2 indicates that the incoming beam enters a convex surface. By keeping R2 fixed at this optimized value, the radius of curvature R4 has been varied until the lowest divergence angle of 0.0446 mrad has been achieved at R4 = - 37 mm. Variation of the divergence angle with R4 is clearly illustrated in figure (3.13). The very small region where the intersection of the curve with the R4 axis takes place has been enlarged as shown in figure (3.14) for the sake of clarification.

The optimized values for R2 and R4 and the corresponding divergence angle of the beam expander optical system are listed in table 3.9.

**Table 3.9 Divergence reduction**.

| Optimized radius of curvature (mm) | Divergence angle (mrad ) |
|---|---|
| R2= 10 | -0.1071221 |
| R4= -37 | -0.0446 |

The final data of the optimized lenses for the beam expander optical system are given in table 3.10. One may deduce that the beam divergence of the system is negligible, which is the aim of the optimization process. The specifications of the beam expander system that give rise to negligible divergence angle are listed in table 3.11. This system is suitable for operation at the wavelength 1.06 μm in the invisible region of the electromagnetic spectrum.

**Table 3.10 Final lens data (all dimensions are in millimeter).**

| Surface | Radius | Thickness | Glass | Semi-Diameter |
|---|---|---|---|---|
| **OBJ** | Infinity | Infinity | | 0 |
| **STO** | Infinity | 10 | | 2.5 |
| **2** | Infinity | 2 | BK7 | 3.5 |
| **3** | 10 | 50 | | 3.5 |
| **4** | Infinity | 5 | BK7 | 13 |
| **5** | -37 | 50 | | 13 |
| **IMA** | Infinity | | | 9.505541 |

**Table 3.11 General lens data**

| | |
|---|---|
| **Number of surfaces** | 6 |
| **Stop number** | 1 |
| **Lens units Millimeter** | **Millimeter** |
| **System aperture** | **5** |
| **Glass catalog** | **Infrared OLD-SCHO** |
| **Effective focal length** | **56104.02** |
| **Back focal length** | **207657.9** |
| **Total track** | **117** |
| **f-number F/#** | **11220.8** |
| **Numerical aperture NA** | **4.456009*10-5** |
| **Stop radius** | **2.5** |
| **Entrance pupil diameter** | **5** |
| **Entrance pupil position** | **0 mm** |
| **Exit pupil diameter** | **18.53798** |
| **Exit pupil position** | **403.13** |
| **Wavelength** | **1.0641 μm** |

Figure 3.15 depicts the spot diagrams of the optimized beam expander system. The intensity profile is drawn adjacent to the interferogram (figure 3.15a). It is seen from figure(3.16c) that the 3-D diagram of the wave front profile is free of distortion at its edge. Hence advantage may be taken from the whole diameter of the spot shown in figure (3.15b). The unchanging spot shape over a distance of 5 km suggests that the proposed beam expander optical system has gained all credibility.

### 3.2.2 Paraxial lens formulas

A procedure similar to that performed on the beam compressor optical system has been carried out here regarding the calculation of the beam expander optical system parameters. The calculations have been performed with the aid of a MATLAB program using the paraxial lens formulas. The various calculated parameters have been compared with those determined by Zemax program for checking the accuracy of the present work and the results are written in table (3.12).

**Table (3.12)**

| **Paraxial lens formuls** | **Zemax result** | **MATLAB result** | **Accuracy** |
|---|---|---|---|
| **Effective Focal length** | 56.10402 m | 56.105131 m | The high accuracy |
| **back focal length** | 207.6579m | 207.662017m | The high accuracy |
| **focal-number** | 11220.8 | 11221.026277 | The high accuracy |
| **numerical aperture** | 4.45600*10-5 | 4.45592*10-5 | very small percentage of error. |
| **depth of focus** | 5.359078*108 μm | 5.359294*108 μm | The accuracy of the two values is extremely high. |
| **field of view** | 0.3268402 | 0.3268339 | The percentage error is negligible. |

### 3.2.3 Ray tracing analysis

The paraxial ray tracing analysis includes image height through the surfaces of the beam expander system in the direction of laser propagation and the angles of paraxial rays. The image height and angels of incidence obtained from Zemax program at various surfaces are given in table 3.13.

**Table 3.13 Zemax ray tracing results.**

| Surface | Image Height (mm) | Tracing Angle (rad) |
|---|---|---|
| **OBJ** | Infinity | 0 |
| **STO** | 2.5 | 0 |
| 2 | 2.5 | 0 |
| 3 | 2.5 | 0.1256545 |
| 4 | 8.832919 | 0.0837716 |
| 5 | 9.253254 | -0.0000446 |
| IMA | 9.251026 | -0.0000446 |

Results concerning the image height and tracing angle have been obtained by using equations (1.11) – (1.13) with the aid of a Matlab software program. These results are listed in table 3.12. A comparison between the results given in tables 3.13 and 3.14 indicates that there is a very high accuracy. Therefore, one may conclude that the results concerning various parameters are verified.

**Table 3.14 Calculated ray tracing results**

| Surface | Image Height (mm) | Tracing Angle (rad) |
|---|---|---|
| **OBJ** | Infinity | 0 |
| **STO** | 2.5 | 0 |
| **2** | 2.5 | 0 |
| **3** | 2.5 | 0.126658 |
| **4** | 8.8329 | 0.084067 |
| **5** | 9.2533 | -4.455920*10-5 |
| **IMA** | 9.2510 | -4.455920*10- |

## 3.3 Optical Systems for Range Finder

Figures 3.16 and 3.17 show the solid model and the shaded model for both optimized beam compressor and beam expander optical systems respectively. Projections of these systems at +20o and –20o with the vertical axis are also illustrated. The dimensions and the constituents of the two systems indicate they are feasible. If the two optical systems that have been achieved in the present work are constructed they may be assembled as small units forming parts of a range finder device. Figure 3.18 illustrates a practical range finder device that may house the suggested beam compressor and beam expander systems.

## 4. Conclusions

1. It appears from the suggested designs cited that the beam expander and beam compressor optical systems for a laser range finder have new specifications achieved by the optimization approach using the Zemax software. The optimization process that has been conducted in the present investigation proved to be a favourable approach for determining optimum radii of curvatures for various lenses in an optical system.
2. The beam expander and beam compressor that have been put forward are intended to be operated in the infrared region of the spectrum. The suggested systems are suitable for a range finder using Nd:YAG laser beam source and lenses of BK7 crown glass.
3. The spot image to be projected on the detector surface by the beam compressor is found to have a radius as small as 54.7 μm with very little aberrations, which have been mainly dominated by spherical aberration.
4. As indicated by the optimized systems, the spot size shape remains unchanged when distant targets are aimed.
5. obtained by Zemax are found to be in good agreement with those determined by Matlab computer program.
6. The dimensions and specifications of the optimized beam compressor and beam expander indicate that these optical systems are feasible.

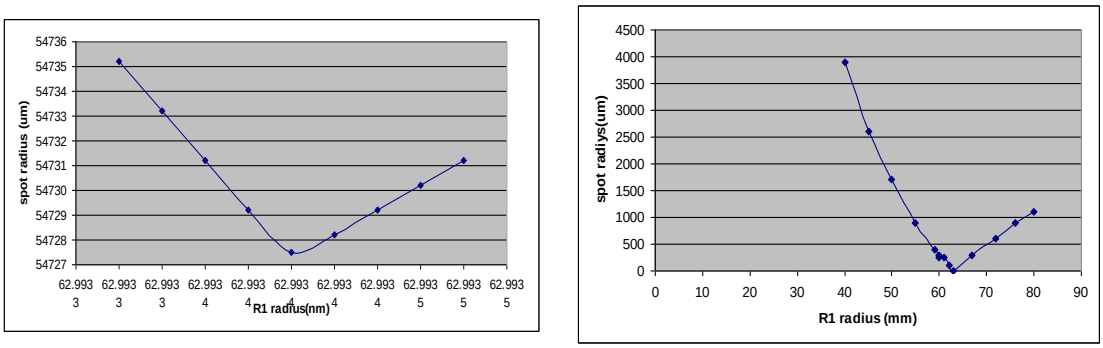


***Figure 3.1 Optimization curve for R1.***

1

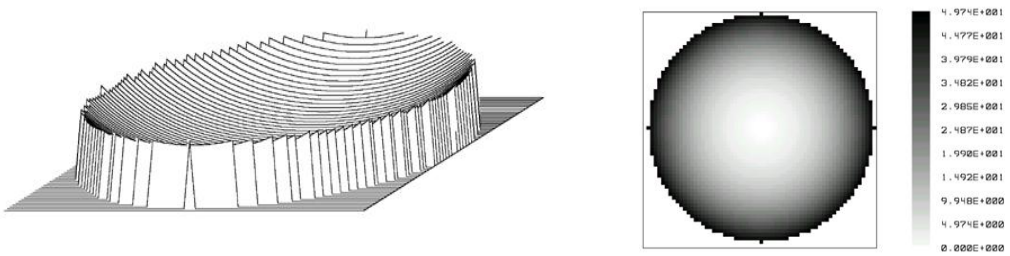

**(a) Spot surface shape** **(b) Gray scale pattern**

***Figure( 3.2) Minimum spot size diagram after the optimization of R1***

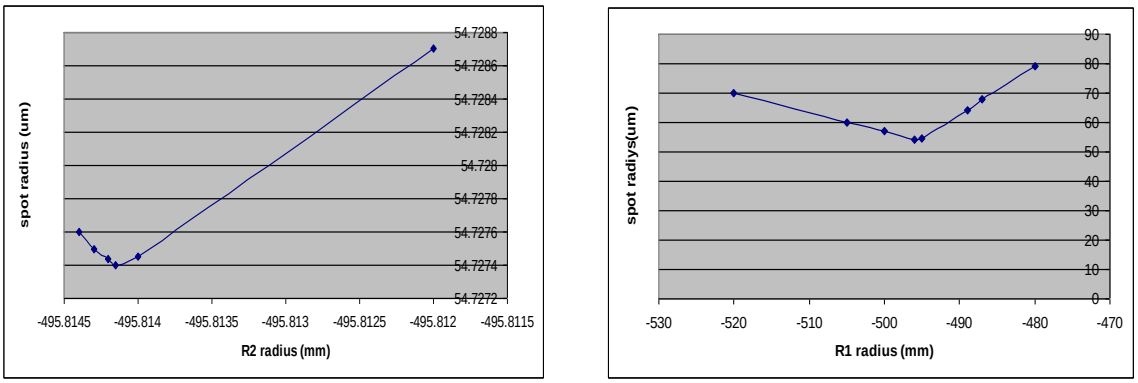


***Figure 3.3 Optimization curve for R2***

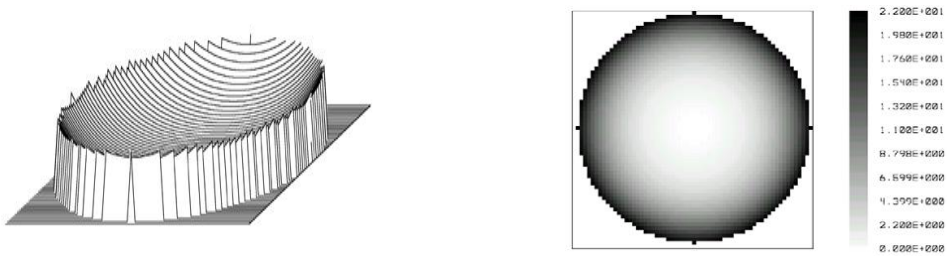

**(a) Spot surface shape** **(b) Gray scale pattern**

***Figure (3.4) Minimum spot size diagram after the optimization of R2.***

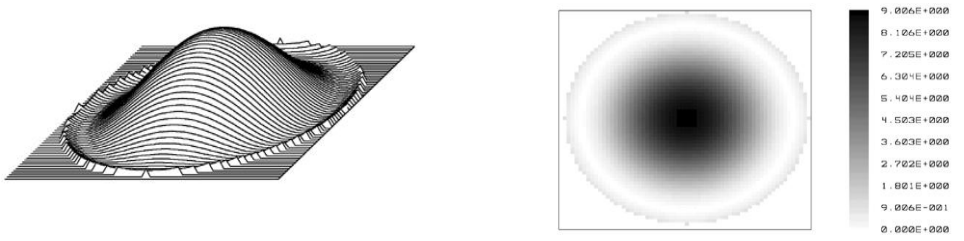

**(a) Spot surface shape** **(b) Gray scale pattern**

***Figure (3.5) Minimum spot size diagram after the optimization of R3.***

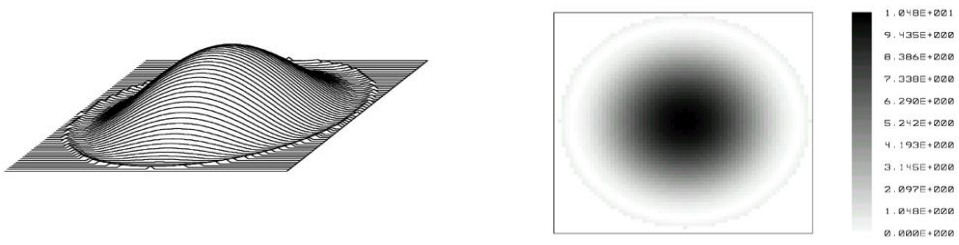

**(a) Spot surface shape** **(b) Gray scale pattern**

***Figure (3.6) Minimum spot size diagram after the optimization of R4.***

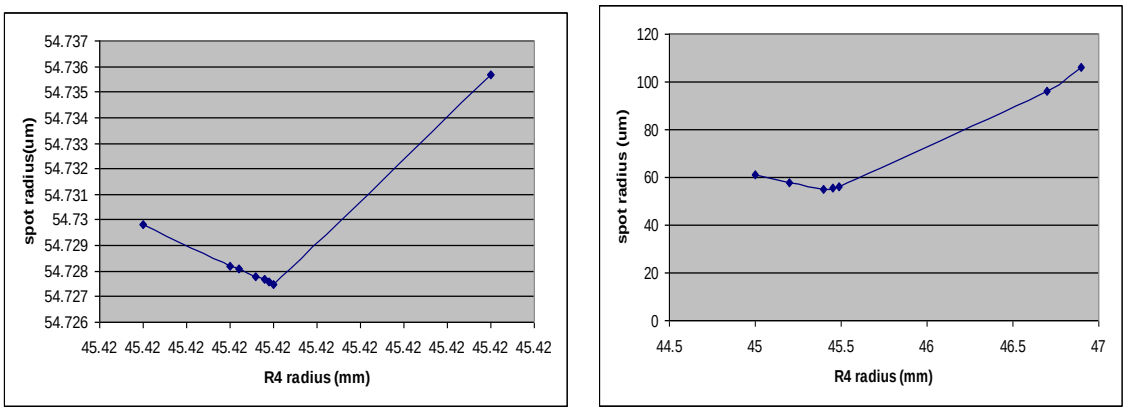


***Figure 3.7 Optimization curve for R4.***

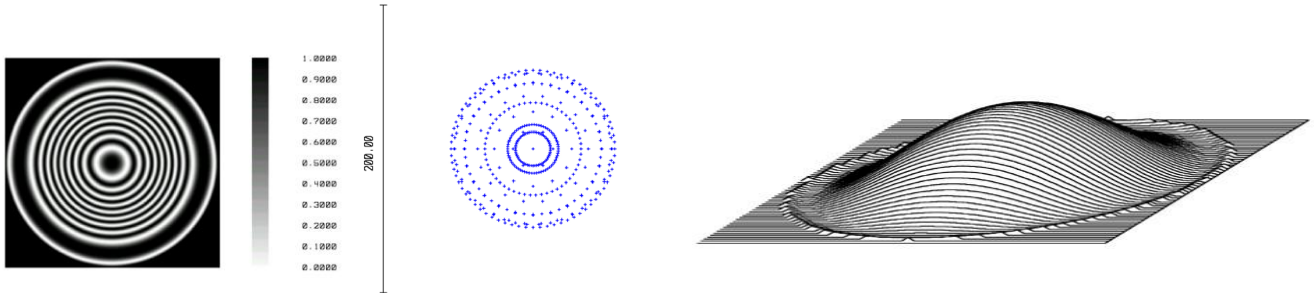

**(a)** **(b)** **( c)**

***Figure(3.8)Spot diagrams (a) interferogram, (b), and (c)wavefront map.***

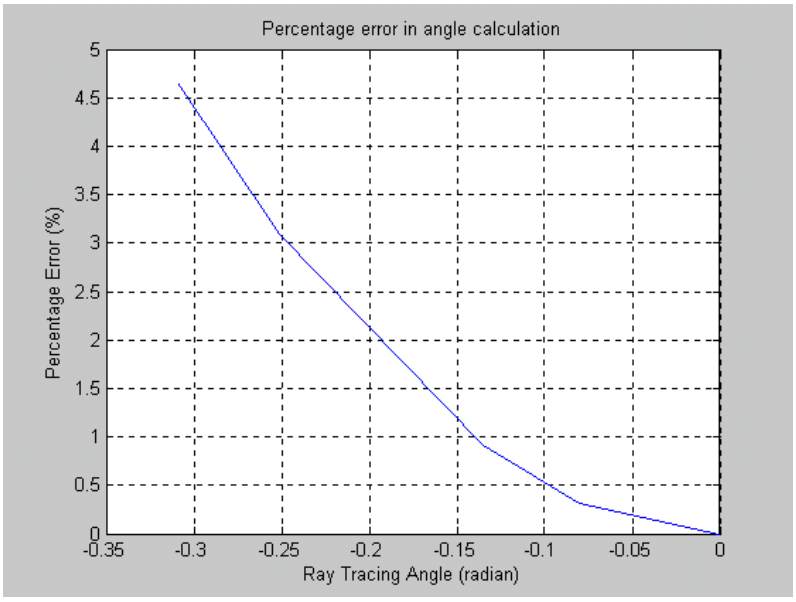


***Figure (3.9) Percentage error as a function of ray tracing angle.***

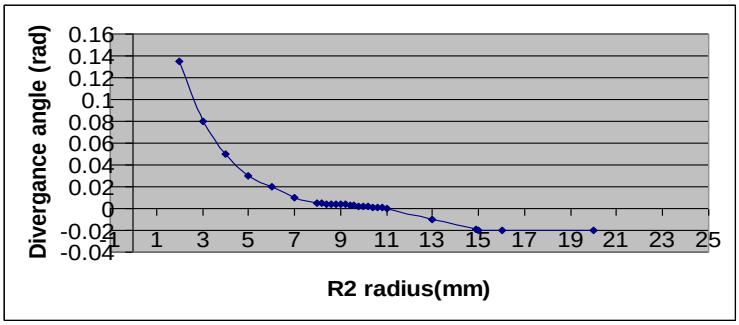


***Figure 3.10 optimization curve for R2***

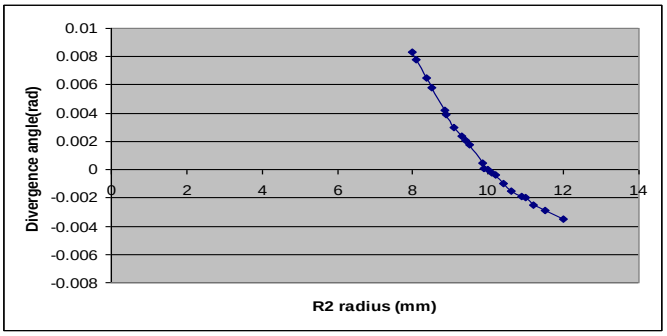


***Figure 3.11 Optimization curve for R2.***

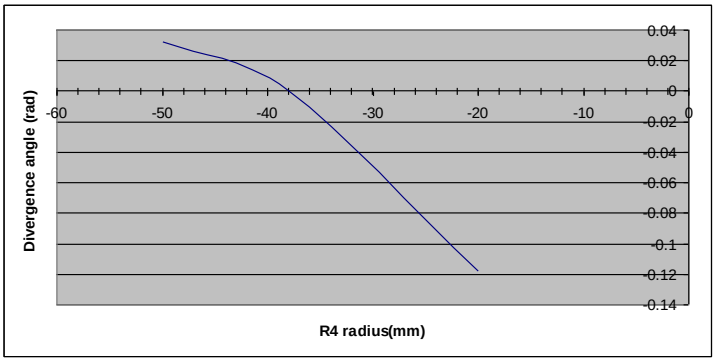


***Figure 3.12 Optimization curve for R4.***

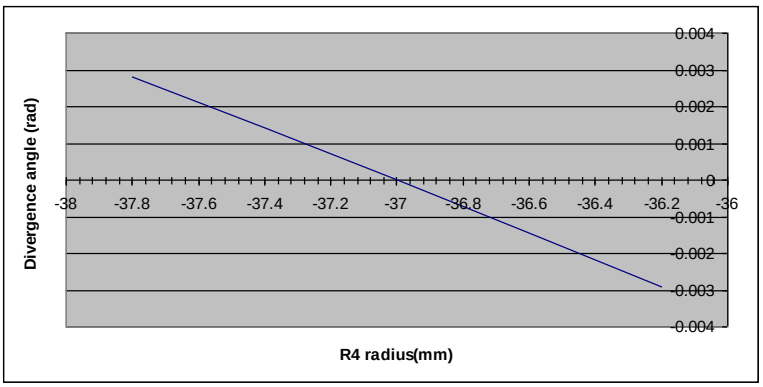


***Figure 3.13 Optimization curve for R4.***

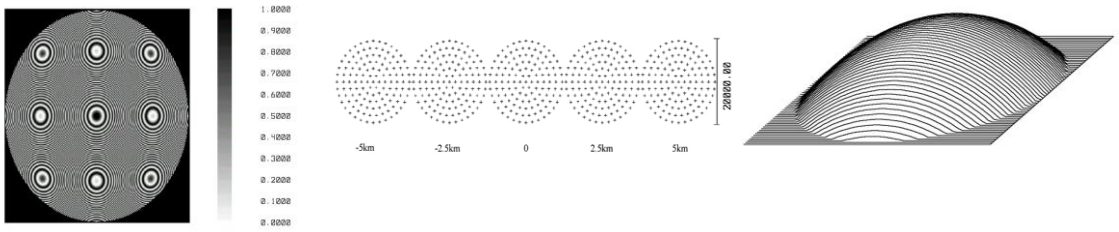


**( a)** **( b)** **(c )**

***Figure 3.14 Spot diagrams (a) interferogram, (b) spot diagram through distance, and (c) wavefront map.***

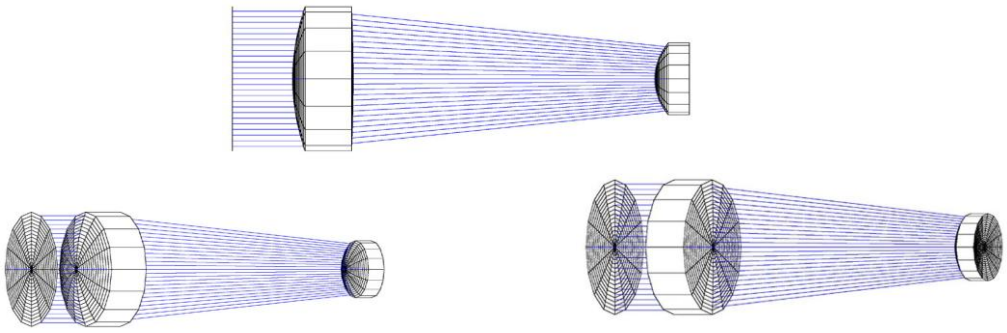

$+20^0$ rotation about vertical axis $-20^0$ rotation about vertical axis

***(a) Solid Model***

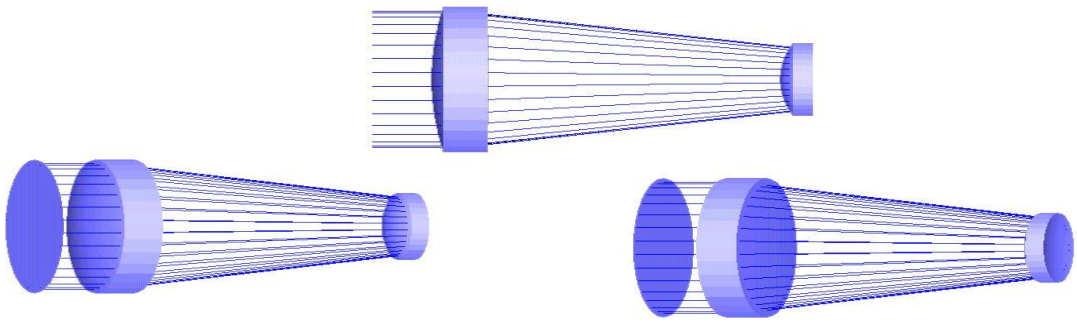

$+20^0$ rotation about vertical axis $-20^0$ rotation about vertical axis

**(b) Shaded Model**

***Figure 3.15 Solid model (a) and shaded model (b) for the optimized beam compressor with +20o and –20o rotation about the vertical axis.***

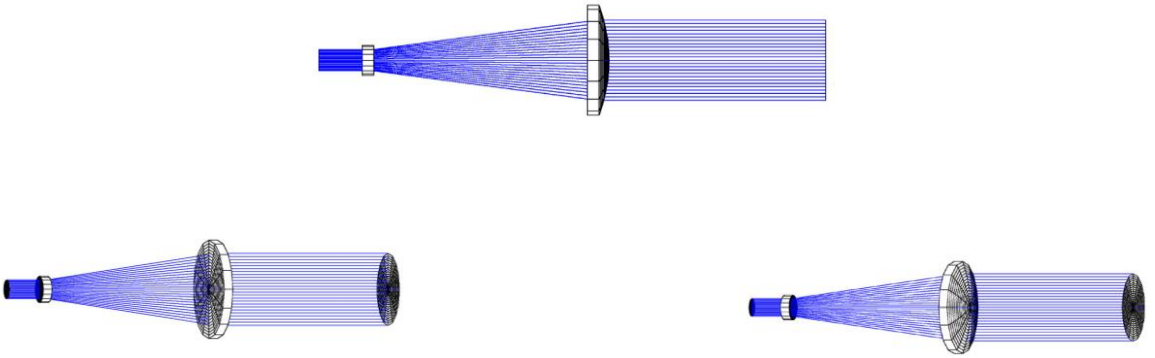

$+20^0$ rotation about vertical axis $-20^0$ rotation about vertical axis

***(a) Solid Model***

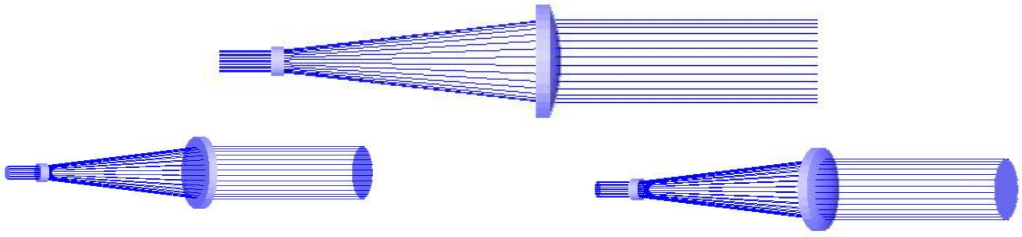

$+20^0$ rotation about vertical axis $-20^0$ rotation about vertical axis

***(b) Shaded Model***

***Figure 3.16 Solid model (a) and shaded model (b) for the optimized beam expander with +20o and –20o rotation about the vertical axis***

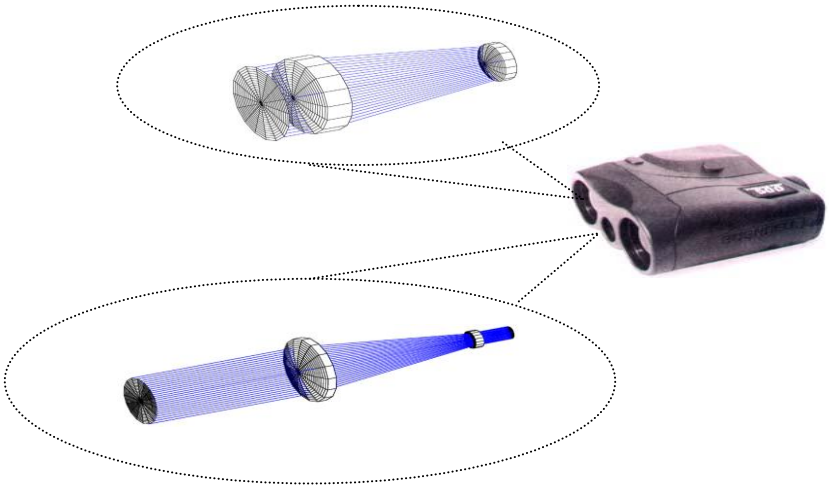

***Figure 3.17 A practical range finder unit that may house the suggested optical systems.***

## REFERENCES

**[1]** P. Thomas, "An Infrared Laser Range Finder", B.Sc. Dissertation, College of Engineering, University of Queensland, (1999).

**[2]** ZEMAX Optical Design Program , User's Guide, Version 8.0, (Focus Software, USA), pp 1-2, 19, and 36, (March 1999).

**[3]** "Fundamental Optics", Via Internet: http//www.mellesgriot.com, (2000).

**[4]** M. Laikin ,"Lens Design", (Marcel Dekker,Inc: New York), (2001).

**[5]** E. Hecht, "Theory and Problems of Optics", (McGraw-Hill Book Company: New York), pp 57-59, Schaum's Outline Series, (1975).

**[6]**"Introduction to Optical Design", From Internet: http://www.Zemax.com/Zemax/Lens Design

**[7]** E. Hecht, "Optics", 3rd ed., (Addison Wesley) p101,257, (1998).

**[8]** R. R. Shannon, "The Art and Science of Optical Design", (Cambridge, University Press, United Kingdom), p 1,6, (1997).

**[9]** W. T. Welford, "Aberration of the Symmetrical Optical Systems", (Academic Press: London), pp 11-12,41-42, (1974).